

Peristaltic Pumping of Bingham Plastic Fluid through a non-uniform Channel

Dr. Uday Raj Singh¹, Uma Shanker²

¹Associate Professor, Department of Mathematics, C.L. Jain (P.G.) College, Firozabad, U.P. (India)

²Research Scholar, Department of Mathematics, C.L. Jain (P.G.) College, Firozabad, U.P. (India)

Abstract- Under lengthy frequency and low Reynolds number estimate, we research the stream brought about by sinusoidal non-uniform peristaltic movement of the cylinder divider in a non-Newtonian liquid complying with Bingham Plastic condition. Both subjective and quantitative conversation and correlations of the discoveries for stream rate, pressure drop and rubbing force are given. The strain inclination ($\partial p/\partial x$) increments with the yield pressure, however diminishes with the rising wave number (δ) and point between channel dividers (α). The conditions for axial velocity, pressure gradient, rubbing friction force, and pressure difference have been determined. With the guide of MATLAB, mathematical and computational outcomes for pressure gradient, angle between walls, amplitude ratio, and wave number are introduced.

Keywords: Bingham Plastic, Reynolds Number, Friction Force, Pressure Gradient, Wave number, amplitude ratio

1. General Prologue-

The dynamic wave compression and development of liquid stream is called peristalsis. This system of liquid stream happens in different pieces of the human body. The rounded construction of muscles in the body shows a peristaltic system. Peristalsis is seen in the improvement of boluses through the throat, undeveloped organism transport inside the urinary parcel. Various analysts concentrate on the significance of peristaltic transport in Newtonian and non-Newtonian liquids.

Considering this, Medhavi (2008) managed the progression of a unique kind of a non-Newtonian liquid complying with the Herschel-Bulkley condition. It is to take note of that Herschel-Bulkley condition can be diminished to numerical models which depict the way of behaving of Bingham, power-regulation and Newtonian liquids for specific selection of boundaries included. Hariharan et al. (2008) examined the peristaltic transport of non-Newtonian liquid, demonstrated as power regulation and Bingham liquid, in a veering tube with various divider wave structures: sinusoidal, multi-sinusoidal, three-sided, trapezoidal and square waves. The convection strategy over peristaltic transport streaming by means of a topsy-turvy channel is considered by Srinivas et al (2009). Singh and Singh (2014) did the investigation of peristaltic stream in a cylinder considering the non-Newtonian liquid: Rabinowitsch liquid model. Chaube et al. (2015) explored peristaltic transport of force regulation liquid in a nonuniform channel under a slip limit condition. They explored the impacts of slip boundary, liquid conduct record, point between the dividers, and wave number on siphoning attributes and catching peculiarity mathematically and portrayed graphically. Yasodhara et al. (2020) investigated the hypothetical examination of peristaltic movement of a non-Newtonian liquid went with in a level channel with flexible dividers. They concentrated on distortion in the dividers of the channel under two viewpoints, one is peristalsis and another is flexibility. Chakradhar et al. (2020) considered peristaltic development of Williamson liquid in a slanted channel, as indicated by suppositions of a low Reynolds number and long frequency. They concentrated on the stream in a wave outline that moves with the speed of the wave. The non-Newtonian liquid models incorporate an examination to look at these variable boundaries and are created by specialists by utilizing Jeffrey (Divya et al., 2020) Bingham, (Comparini and Mannucc, 1998) and Rabinowitsch (Vaidya et al., 2019) liquid models. The warm conductivity and thickness are considered as factors for the capacity of temperature. Venthan et al. (2021) concentrated on the progression of Bingham nano fluids at the entrance segment working as non-Newtonian nanofluids in barrel shaped concentric rollers.

2. Formulation of Problem –

A hydrodynamic slip limit condition constrains the peristaltic flow of Bingham Plastic fluid in a non-uniform channel. Let a non-uniform sinusoidal wave drive the channel's dividers forward and backward in time.

Transverse vibration of the wall (h)

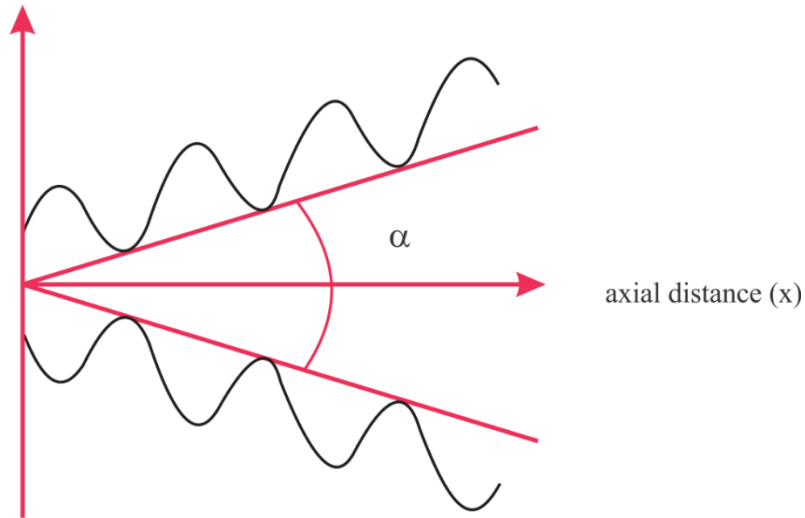


Figure 1-Configuration of a peristaltic channel that is not uniform

$$H = a + x \tan\alpha + b \sin\alpha \quad (1)$$

$$-\frac{\partial p}{\partial x} = \frac{1}{r} \frac{\partial}{\partial r} (r\tau) + \frac{\sin\alpha}{F} \quad (2)$$

$$\begin{cases} -\frac{\partial w}{\partial r} = f(\tau) = \left(\frac{\tau - \tau_0}{k}\right) & \tau \geq \tau_0 \\ \frac{\partial w}{\partial r} = f(\tau) = 0 & \tau \leq \tau_0 \end{cases} \quad (3)$$

$$-\frac{\partial w}{\partial r} = f(\tau) = \left(\frac{\tau - \tau_0}{k}\right); \tau \geq \tau_0$$

A presentation of the accompanying non-layered factors

$$r' = \frac{r}{a}, x' = \frac{x}{\lambda}, t' = \frac{ct}{\lambda}, u' = \frac{u}{c}, \tau'_0 = (a/c\lambda)^{1/n} \tau_0, p' = \left[\frac{a^{n+1}}{c\lambda^n}\right]^{1/n} p \quad (4)$$

$$\begin{cases} -\frac{\partial p}{\partial x} = \frac{1}{r} \frac{\partial}{\partial r} r \left[k \left(-\frac{\partial w}{\partial r} \right) + \tau_0 \right] + \frac{\sin\alpha}{F} & \tau \geq \tau_0 \\ \frac{\partial w}{\partial r} = f(\tau) = 0; & \tau \leq \tau_0 \end{cases} \quad (5)$$

where τ and τ_0 are dimensionless shearing and yield stresses, separately.

The non-layered limit conditions are

$$\begin{cases} w = -1 & \text{at } r = \frac{H}{a} = h = 1 + \frac{x}{\delta} \tan\alpha + \phi \sin 2\pi x \\ \tau \text{ is finite} & \text{at } r = 0 \end{cases} \quad (6)$$

Where $\phi = \frac{b}{a}$

Solving equation (5) using boundary conditions (6), we get

$$w = -1 + \frac{1}{2}(P + f)(r^2 - h^2) + \tau_0(r - h) \quad (7)$$

Where $P = \frac{\partial p}{\partial x}, f = \frac{\sin\alpha}{F}$

The non-dimensional volumetric stream rate in the wave outline is characterized as

$$q = 2 \int_0^h r w dr \quad (8)$$

$$q = -h^2 + \frac{1}{2}\tau_h h^3 - \frac{1}{4}f h^4 + \frac{1}{3}\tau_0 h^3 \quad (9)$$

Where $\tau_h = -\frac{h}{2} \frac{\partial p}{\partial x}$ (10)

From equation (9) and (10), we obtain

$$-\frac{\partial p}{\partial x} = 4 \left[\frac{q}{h^4} + \frac{1}{h^2} + \frac{1}{4}f - \frac{1}{3h}\tau_0 \right] \quad (11)$$

The mean volume flow rate, Q over a period as

$$Q = q + 1 + \frac{\phi^2}{2} \quad (12)$$

From equations (11) and (12),

$$-\frac{\partial p}{\partial x} = 4 \left[\left(Q - 1 - \frac{\phi^2}{2} \right) \frac{1}{h^4} + \frac{1}{h^2} + \frac{1}{4} f - \frac{1}{3h} \tau_0 \right] \quad (13)$$

Since the pressure drop, $\Delta p = p(1) - p(0)$, across one frequency is same whether estimated in moving or fixed coordinate framework, it is thusly determined utilizing condition (13)

$$\begin{aligned} \Delta p &= \int_0^1 \left(-\frac{\partial p}{\partial x} \right) dx \\ &= 4 \int_0^1 \left[\left(Q - 1 - \frac{\phi^2}{2} \right) \frac{1}{h^4} + \frac{1}{h^2} + \frac{1}{4} f - \frac{1}{3h} \tau_0 \right] dx \\ &= 4 \left[\frac{f}{4} + \left(Q - 1 - \frac{\phi^2}{2} \right) \int_0^1 \frac{1}{h^4} dx + \int_0^1 \frac{1}{h^2} dx - \frac{\tau_0}{3} \int_0^1 \frac{1}{h} dx \right] \end{aligned} \quad (14)$$

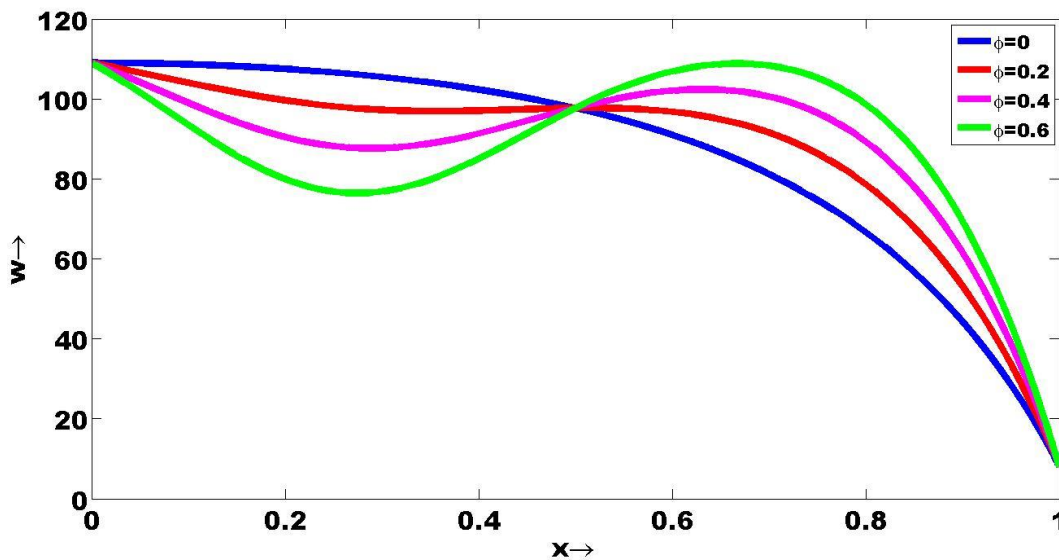
The non-layered erosion force, F is the grinding force at the divider in the fixed direction framework which is same as in moving framework) is along these lines gotten as

$$\begin{aligned} F &= \int_0^1 h^2 \left(-\frac{\partial p}{\partial x} \right) dx \\ &= \int_0^1 4h^2 \left[\frac{q}{h^4} + \frac{1}{h^2} + \frac{1}{4} f - \frac{1}{3h} \tau_0 \right] dx \\ &= \int_0^1 4 \left[1 + \frac{q}{h^2} + \frac{1}{4} f h^2 - \frac{h}{3} \tau_0 \right] dx \end{aligned} \quad (15)$$

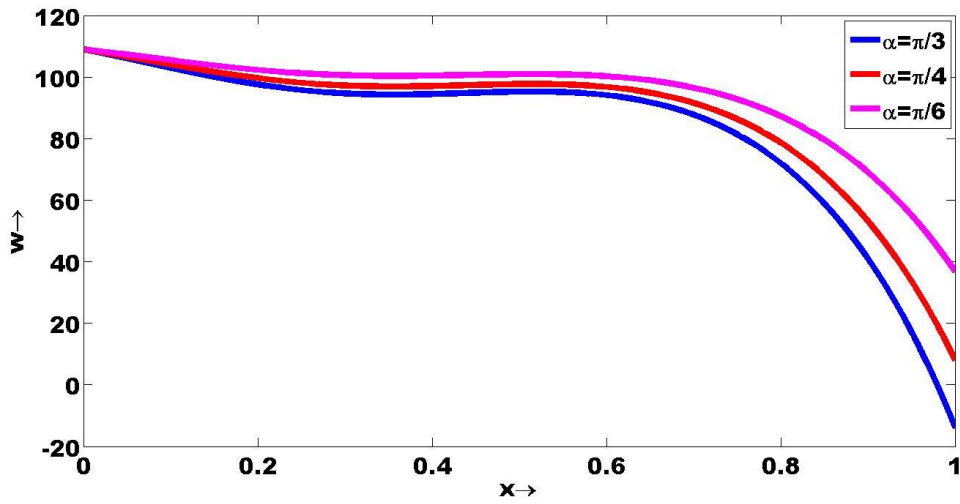
At long last, taking into account the confounded type of the articulation for Δp given in condition (14), it is challenging to get the insightful articulation for the stream rate, Q for zero strain drop. In any case, the strain drop for zero stream rate, $(\Delta p)_{Q=0}$ which is quite compelling is determined as

$$(\Delta p)_{Q=0} = 4 \left[\frac{f}{4} - \left(1 + \frac{\phi^2}{2} \right) \int_0^1 \frac{1}{h^4} dx + \int_0^1 \frac{1}{h^2} dx - \frac{\tau_0}{3} \int_0^1 \frac{1}{h} dx \right] \quad (16)$$

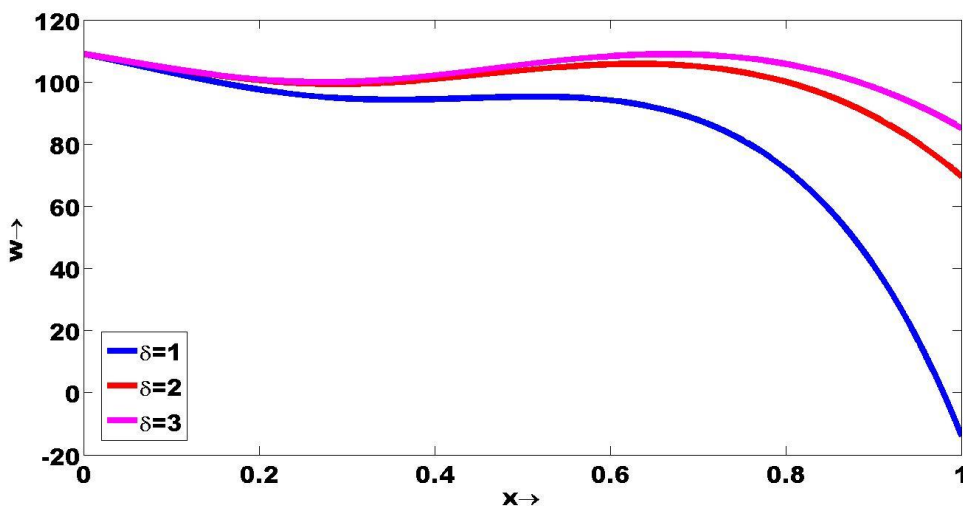
3. Numerical Results and Discussion-



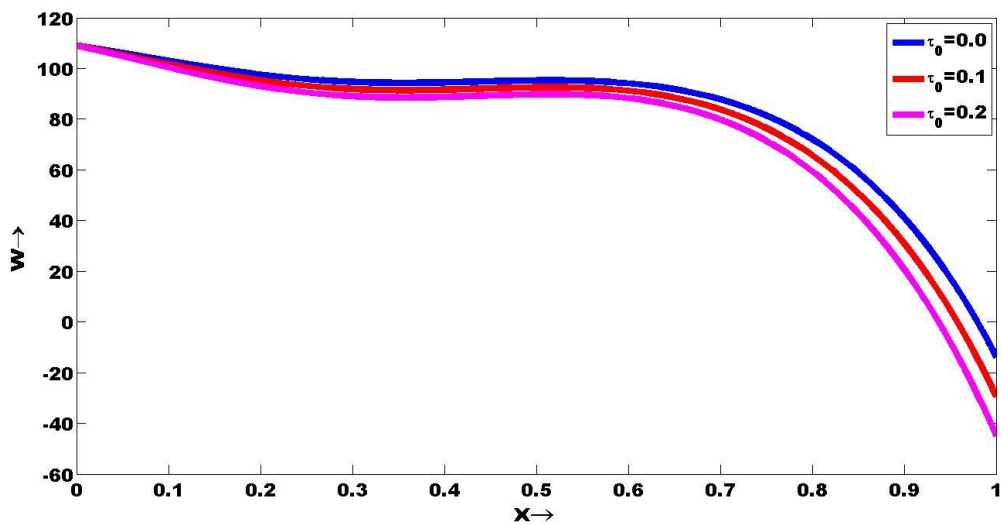
Graph- 1: w with x for different value of ϕ



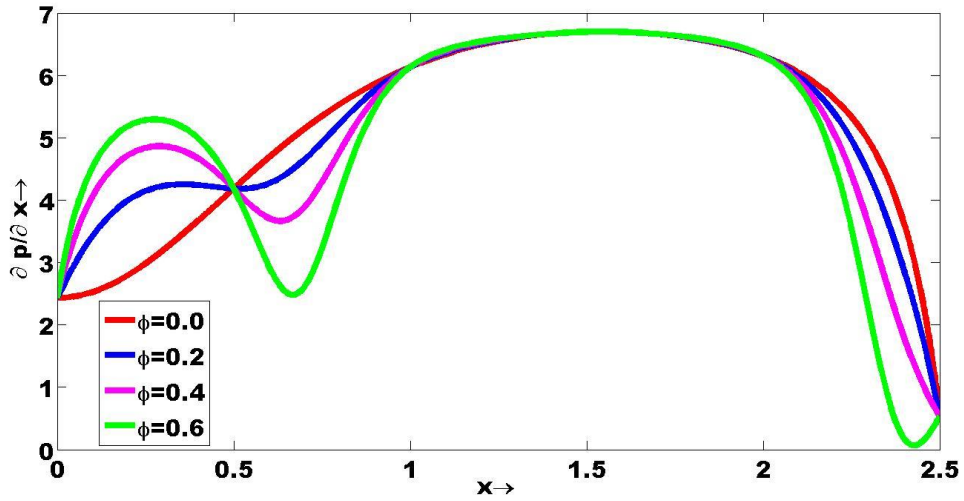
Graph-2: w with x for different value of α



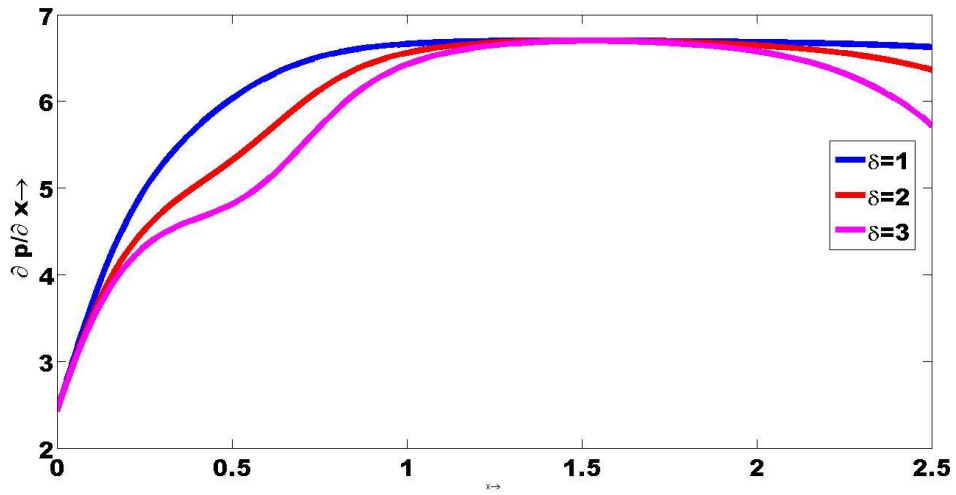
Graph-3: w with x for different value of δ



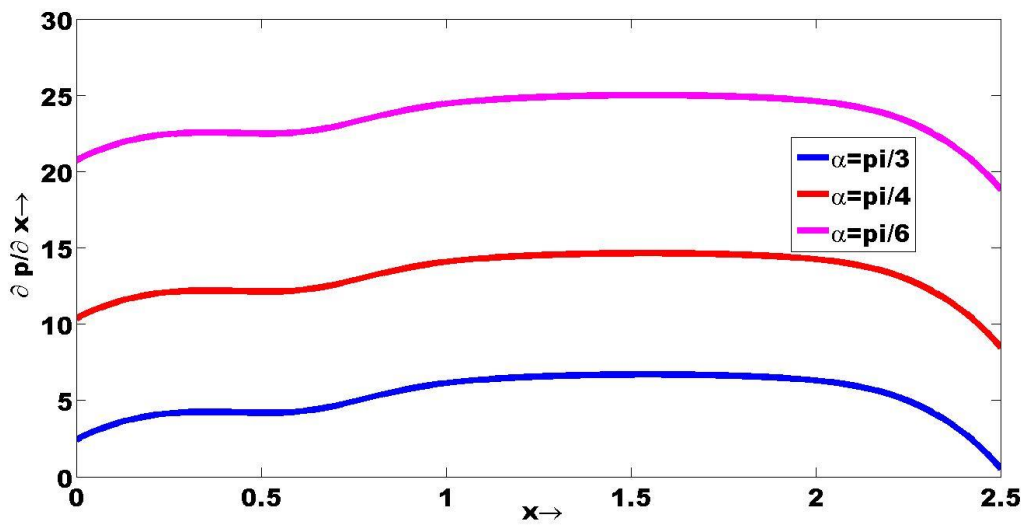
Graph-4: w with x for different value of τ_0



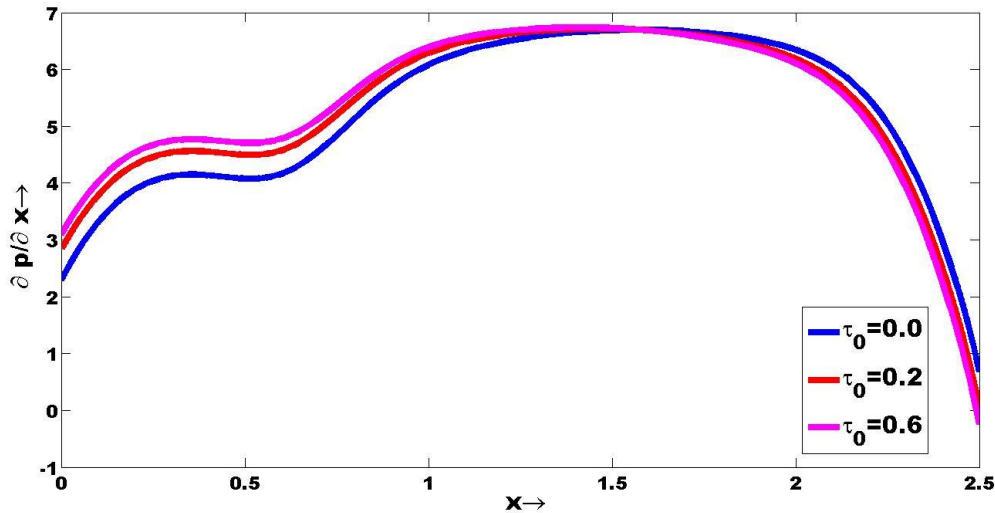
Graph-5: $\frac{\partial p}{\partial x}$ with x for different value of ϕ



Graph-6: $\frac{\partial p}{\partial x}$ with x for different value of δ



Graph-7: $\frac{\partial p}{\partial x}$ with x for different value of α



Graph-8: $\frac{\partial p}{\partial x}$ with x for different value of τ_0

In this segment, mathematical estimations executed on MATLAB programming are introduced by means of diagrams, or at least, Graphs (1-8). We methodically concentrate on the impacts of amplitude ratio (ϕ), angle between the walls (α), wave number (δ) and yield stress (τ_0) on the speed profile (pivotal speed) and pressure gradient. Charts (1)-(4) outline the speed profiles (pivotal speed) versus hub relocation. Chart (1) portrays the speed profile for different upsides of amplitude ratio $\phi = 0, 0.2, 0.4, 0.6$. It is seen from this chart that hub speed diminishes from $x=0$ to $x=0.5$ and increments from $x=0.5$ to $x=1$ as amplitude ratio increments. Chart (2) depicts the speed profile for different upsides of point between the dividers $\alpha = \frac{\pi}{3}, \frac{\pi}{4}, \frac{\pi}{6}$. It is noted from this chart that pivotal speed increments as point between the dividers decreases. Diagram (3) portrays the speed profile for different upsides of wave numbers $\delta = 1, 2, 3$. It is seen from this diagram that hub speed increments as wave number intensifies. Diagram (4) depicts the speed profile for different upsides of yield pressure $\tau_0 = 0, 0.1, 0.2$. It is seen from this diagram that pivotal speed decreases as yield pressure amplifies. Charts (5)- (8) exhibit the speed pressure slope versus pivotal removal. Chart (5) depicts the strain inclination for different upsides of plentifulness proportion. It is seen from this chart that pressure slope increments from $x=0$ to $x=0.5$, diminishes from $x=0.5$ to $x=1$, stays steady from $x=1$ to $x=2$ and again diminishes from $x=2$ to $x=2.5$ as amplitude ratio proportion increments. Chart (6) depicts the strain inclination for different upsides of wave number. It is seen from this chart that pressure slope diminishes as wave number increases. Chart (7) portrays the strain slope for different upsides of point between the dividers. It is seen from this chart that pressure slope diminishes as point between the dividers make more grounded. Chart (8) portrays the tension inclination for different upsides of yield pressure. It is seen from this chart that pressure inclination increments from $x=0$ to $x=1.5$ and diminishes $x=1.5$ to $x=2.5$ as yield pressure improves.

4. Closing Comments-

This research examined the two-dimensional peristaltic flow of a Bingham Plastic physiological fluid through a nonuniform channel. Studies of sinusoidal non-uniform peristaltic waves using long wavelength approximation have been carried out using a model of non-Newtonian fluid obeying the Bingham Plastic equation. There is a distinct difference between friction and pressure rise (negative of pressure drop). Results of this study may be used to discuss the peristaltic-induced flow of blood and other physiological fluids, according to experts. Intestinal flow can be studied using the model presented in this paper. (chyme movement from small intestine to large intestine). It's also relevant to biomimetic pump simulations that transport hazardous materials, polymers, and the like.

REFERENCES:

1. Chakradhar K., Nandagopal K., Sastry T.V.A.P. (2020): "Impact of the Permeable Wall lining on the Peristaltic flow of Williamson fluid in an Inclined Channel", International Journal of Mechanical Production, 10(3): 12675-12688.
2. Chaube M.K., Tripathi D., Beg O.A., Sharma S., Pandey V.S.(2015): "Peristaltic Creeping Flow of Power Law Physiological Fluids through a Nonuniform Channel with Slip Effect", Applied Bionics and Biomechanics, ID 152802, 10 pages.
3. Comparini E, Mannucc P. (1998): Flow of a Bingham fluid in contact with a Newtonian fluid. J Math Anal Appl., 227: 359-381.
4. Divya B.B., Manjunatha G., Rajashekhar C., Vaidya H., Prasad K.V. (2020): "The hemodynamics of variable liquid properties on the MHD peristaltic mechanism of Jeffrey fluid with heat and mass transfer", Alexandria Eng J., 59:693-706.
5. Hariharan P., Seshadri V., Banerjee R.K. (2008): "Peristaltic transport of non-Newtonian fluid in a diverging tube with different wave forms", Mathematical and Computer Modelling, 48: 998-1017
6. Medhavi A. (2008): "Peristaltic Pumping of a Non-Newtonian Fluid", Applications and Applied Mathematics, 3(1):137-148. Rabinowitsch Fluid Model", International Journal of Fluids Engineering, 6(1):1-8.

7. Singh B.K., Singh U.P. (2014): "Analysis of Peristaltic Flow in a Tube:
8. Srinivas S, Gayathri R, Kothandapani M. (2009): "The influence of slip conditions, wall properties and heat transfer on MHD peristaltic transport", *Comput Phys Commun.*,180:2115-2122.
9. Vaidya H., Rajashekhar C., Manjunatha G., Prasad K.V.(2019): "Peristaltic mechanism of a Rabinowitsch fluid in an inclined channel with compliant wall and variable liquid properties" *J Braz Soc Mech Sci Eng.*, 41:52.
10. Venhan M.S., Amalraj I.J., Kumar P.S., Nisha M.S. (2021): "Non-Newtonian nanofluids flow analysis at the ingress section in process intensified system", *Chemical Engineering and Processing-Process Intensification*,167: 108518
11. Yasodhara G., Sreenadh S., Sumalatha B., Srinivas A.N.S. (2020): "Axisymmetric Peristaltic Flow of a Non-Newtonian Fluid in a Channel with Elastic Walls", *Mathematical Modeling of Engineering Problems*, 7(2): 315-323.